Inorg. Chem. **2006**, *45*, 2022–2026

Crystal Structure and Physical Properties of $Fe_{1.5}Pb_{5.5}In_{10}S_{22}$

Yoshitaka Matsushita* and Yutaka Ueda

Materials Design and Characterization Laboratory (MDCL), Institute for Solid State Physics (ISSP), The University of Tokyo, 5-1-5 Kashiwanoha, Kashiwa, Chiba 277-8581, Japan

Received September 8, 2005

A new compound, $Fe^{2+}_{1.5}Pb^{2+}_{5.5}In^{3+}_{10}S^{2-}_{22}$, was found in the Fe–Pb–In–S system. The crystals had a shiny metallic gray luster and were obtained in a barlike shape. The melting and recrystallizing points are 1098 and 1090 K, respectively. The crystal structure determined by X-ray diffraction is $P2/m$, $a = 14.558(1)$ Å, $b = 3.8556(3)$ Å, $c = 15.558(1)$ Å, $\beta = 96.876(1)°$, $V = 867.0(1)$ Å^3, $Z = 1$, $D_c = 5.893$ g/cm^3, and R1 = 3.78%, which is an isostructure with $Sn_{5.5}In_{11}S_{22}$. In the structure, lead atoms exist at three crystallographically independent sites, and one of them, Pb1, is occupied by a quarter of indium atoms. All of the Fe ions are randomly distributed at six indium sites. This compound is a semiconductor with a band gap, $E_a = 0.95$ eV. The dominant magnetic interaction is antiferromagnetic, but magnetic orderings are not observed down to 2 K.

Introduction

The diverse structural chemistry and electromagnetic properties exhibited by metal chalcogenides lead to important opportunities for these materials in contemporary electronic device research.[1] Recent research efforts on metal chalcogenides focus on improved transistors,[1] solar cells,[1] thermoelectrics,[2] solid-state electrolytes for lithium secondary batteries,[3] and memory materials.[4] As one of the accessible commercial applications, optical disks based on "Ge−Sb−Te" phase-change materials are rapidly increasing in the current DVD-RW markets.[4] In the III−V system, the diluted magnetic semiconductors such as (In, Mn)As[5a] or (Ga, Mn)-As[5b] open up the emerging spintronics field for electronic devices with the amazing possibility of using spin freedom of charge carriers.[5c] However, their magnetic transition temperatures are too low for practical applications (i.e., $T_{curie} = 110$ K in (Ga, Mn)As[5d]). In 2003, Saito and coworkers found a new diluted magnetic chalcogenide semiconductor, (Zn, Cr)Te which showed ferromagnetism at room temperature.[6]

We have studied multinary chalcogenids with transition metals in anticipation of an exciting new magnetophenomena from the local dimensionalities and environments of the elements.[7] In the fields of magnetochemistry and magnetophysics, low-dimensional magnetic compounds have drawn great interest because of their peculiar properties which are caused by the quantum many body effects. Particularly, one-dimensional Heisenberg antiferromagnetic chain (1D-HAF) compounds have been extensively researched because most of them are considered to be a prototype in statistic physics. An example of a 1D-HAF system is the Haldane system. In 1983, Haldane theoretically predicted that the 1D-HAF system with an integer spin quantum number ($S = 1, 2, ...$) should have a spin-energy gap, the Haldane gap (Δ), between the ground state and the first excited state. On the other hand, in the case of half-integer spin quantum number ($S = 1/2, 3/2, ...$) systems, the energy levels are have no spin gap.[8]

* To whom correspondence should be addressed. E-mail: chaos@issp.u-tokyo.ac.jp.

(1) Matsumoto, T.; Takizawa, T.; Shirakata, S.; Wada, T.; Yamamoto, N., Eds. *Japanese Research Review for Pioneering Ternary and Multinary Compounds in the 21st Century*; Institute of Pure and Applied Physics (IPAP): Tokyo, 2001.

(2) (a) Rowe, D. M., Ed. *CRC Handbook of Thermoelectrics*; CRC Press: Boca Raton, FL, 1995. (b) Kanatzidis, M. G. *Semicond. Semimet.* **2001**, *69*, 51. (c) Chung, D.-Y.; Hogan, T.; Brazis, P.; Rocci-Lane, M.; Kannewurf, C.; Bastea, M.; Uher, C.; Kanatzidis, M. G. *Science* **2000**, *287*, 1024.

(3) (a) Matsushita, Y.; Kanatzidis, M. G. *Z. Naturforsch.* **1998**, *53b*, 23. (b) Kanno, R.; Hata, T.; Kawamoto, Y.; Irie, M. *Solid State Ionics* **2000**, *130*, 97.

(4) Ushkov, B.; Fairman, R., Eds. *Semiconducting Chalcogenide Glass*; Academic Press: Orlando, FL, 2004; Vols. 1−3.

(5) (a) Munekawa, H.; Ohno, H.; von Molnar, S.; Segmüler, A.; Chang, L. L.; Esaki, L. *Phys. Rev. Lett.* **1989**, *63*, 1849. (b) Ohno, H. *Science* **1998**, *281*, 951. (c) Prinz, G. A. *Science* **1998**, *282*, 1660. (d) Matsukura, F.; Ohno, H.; Shen, A.; Sugawara, Y. *Phys. Rev.* **1998**, *B*57, R2037.

(6) Saito, H.; Zayets, V.; Yamagata, S.; Ando, K. *Phys. Rev. Lett.* **2003**, *90*, 207202.

(7) (a) Matsushita, Y.; Ueda, Y. *Inorg. Chem.* **2003**, *42*, 7830. (b) Matsushita, Y.; Ueda, Y. *Prog. Theor. Phys. Suppl.* **2005**, *159*, 179.

(8) (a) Haldane, F.D.M. *Phys. Rev. Lett.* **1983**, *50*, 1153. (b) Katsumata, K. *Curr. Opin. Solid State Mater. Sci.* **1997**, *2*, 226 and references therein.

10.1021/ic0515296 CCC: $33.50
Published on Web 02/03/2006

Recently, the magnetic properties of a 1D-HAF compound with a rare $S = 2$, $FePb_4Sb_6S_{14}$, were reported.[7,9] The compound has an isolated 1D straight chains of Fe^{2+} ($S = 2$). Unfortunately, such Haldane gap behavior has not been observed in this compound, and Léone et al. reported instead that the ground state of this compound was an antiferromagnetic long-range order from the results of low-temperature neutron powder diffraction using a natural mineral sample.[9] On the other hand, we observed a spin-glass behavior in ac magnetic-susceptibility measurements using our synthetic sample.[7] In the current research, we tried to substitute In^{3+} for Sb^{3+} because the magnetic interaction would be varied by the substitution of the ion with somewhat different ionic radius: $r_{Sb^{3+}}^{CN=6} = 0.76$ Å and $r_{In^{3+}}^{CN=6} = 0.80$ Å.[10] However, we could not obtain the $FePb_4In_6S_{14}$ phase, but we found a new compound, $Fe_{1.5}Pb_{5.5}In_{10}S_{22}$. In this paper, we report the crystal structure and physical properties of this new compound, $Fe_{1.5}Pb_{5.5}In_{10}S_{22}$.

Experimental Section

Synthesis. $Fe_{1.5}Pb_{5.5}In_{10}S_{22}$ was synthesized by a solid-state reaction using FeS (3 N, powder, CERAC Ltd.), Pb (5 N+, shot, Rare-Metallic Ltd.), In_2S_3 (3 N, lump, Kojundo Kagaku, Co.), and S (5 N, shot, Rare-Metallic Ltd.). These starting materials were roughly mixed in the ratio of 1:3:2.5:3 FeS/Pb/In_2S_3/S, and the mixture was sealed into an evacuated silica tube ($\sim 10^{-5}$ Torr). The mixture was slowly heated to 1123 K over 12 h, isothermed at this temperature for 3 days, cooled to 673 K over 100 hrs, and then cooled to room temperature within 10 h. Bar-shaped shiny metallic silver crystals were obtained. The maximum size of a crystal is $0.3 \times 0.3 \times 2.0$ mm, while a typical size is $0.05 \times 0.05 \times 0.5$ mm. Both ball-shaped PbS impurities and chunk $PbIn_2S_4$ impurities were observed in the products.

Characterization. The phase identification of prepared samples was done by powder X-ray diffraction (XRD) using a Mac Science M21X (Cu Kα radiation, 45 kV, 350 mA) instrument. The observation of crystal morphology and the composition analysis were performed by using a JEOL JSM-5600 scanning electron microscope (SEM) with a wavelength-dispersive spectrometer (WDS) analyzer at a 15 kV accelerating voltage and a 1 min accumulation time per position, in which the corrections were made for atomic number, absorption, and fluorescence. The samples used for physical property measurements were carefully checked to ensure that they were homogeneous before the measurements were performed.

Differential Thermal Analysis. Differential thermal analysis was performed with a Mac Science TG-DTA 2000 thermal analyzer. The crystals were sealed in a silica ampule under vacuum ($\sim 10^{-5}$ Torr). An almost equal mass of α-Al_2O_3 sealed into an evacuated ampule was used as a reference. DTA curves were measured at a heating and cooling rate of 10 K/min between room temperature and 1143 K. After the DTA measurements, the samples were checked by XRD.

Crystallographic Study. The powder XRD measurements suggest a structure similar to that of $Sn_{5.5}In_{11}S_{22}$[13]. Before the intensity data collection for the X-ray crystal structure determination, needle crystals were confirmed to grow along the *b* axis of the $Sn_{5.5}In_{11}S_{22}$-type structure, from the oscillation photographs using Mo Kα X-ray ($\lambda = 0.71069$ Å) at room temperature. The chemical composition was estimated to be $Fe_{1.37(2)}Pb_{5.58(3)}In_{10.10(3)}S_{22}$ by WDS measurements at about 20 different positions in a crystal. A needle crystal with a dimension of $0.025 \times 0.025 \times 0.150$ mm^3 was selected for intensity data collection. Intensity data at 296 K were collected in the full sphere region up to $2\theta = 60°$ on a Bruker SMART-APEX CCD-based diffractometer equipped with a pyrolitic graphite monochromator and Mo Kα radiation (40 kV, 130 mA). No crystal decay was detected during the measurements. SMART software was used for data collection, and SAINT was used for data extraction and reduction.[11a] The absorption correction was performed empirically using SADABS.[11b] The initial structure was solved by direct methods[11c] and refined by full-matrix least-squares techniques on F^2 using the teXsan package.[11d] The final cycle of refinement performed on F_o^2 with 129 variables and 2181 averaged reflections [$F_o^2 > 2\sigma(F_o^2)$] converged to residual wR2 = 0.0674 and R1 = 0.0378. The crystallographic information and the results of refinement are given in Table 1, and selected bond distances are given in Table 2. The crystal structures were drawn by CrystalMaker.[11e]

Table 1. Crystallographic Data and Structural Analysis for $Fe_{1.50}Pb_{5.50}In_{10}S_{22}$

fw	3076.89
cryst shape/color	needle/metallic gray
temp	296 K
space group	*P*2/*m* (#10)
a	14.558(1) Å
b	3.8556(3) Å
c	15.558(1) Å
β	96.876(1)°
V	867.0(1) Å^3
Z	1
D_c	5.893 g/cm^3
F_{000}	1332
μ(Mo Kα)	35.068 mm^{-1}
no. measured reflns	8842
no. unique reflns	2530
no. obsd reflns [$F_o^2 > 2.0\sigma(F_o^2)$]	2181
R_{int}	4.3%
final R1/wR2 [$F_o^2 > 2.0\sigma(F_o^2)$]	3.78/6.74%
GOF	1.448

Charge-Transport Measurements. The dc electrical resistivity along the *b* axis of a single crystal was measured using the usual four-probe technique. The electrodes, ø25 μm gold wires, were attached to the crystal using gold pastes. Measurements were carried out in the temperature range of 70−300 K by a Quantum Design PPMS with an ac transport controller. However, below 200 K, we could not obtain realistic data because the resistivity of the sample was too high for our instrument.

Magnetic Measurements. Magnetic susceptibility for pure polycrystalline material was measured in the temperature range of 2−350 K at an applied magnetic field of 0.5 T with zero-field-cooling (ZFC) and field-cooling (FC) modes using a Quantum Design 5T-MPMS SQUID magnetometer. For the measurements, the sample was wrapped with a polyethylene sheet. Data were corrected for background.

(9) (a) Léone, P.; Le Leuch, L. M.; Palvadeau, P.; Molinié, P.; Moëlo, Y. *Solid State Sci.* **2003**, *5*, 771. (b) Léone, P.; André, G.; Doussier, C.; Moëlo, Y. *J. Magn. Magn. Mater.* **2004**, *284*, 92.

(10) Shannon, R. D. *Acta Crystallogr.* **1976**, *A32*, 751.

(11) (a) *SMART* and *SAINT*, version 5; Siemens Analytical X-ray System, Inc.: Madison, WI, 1998. (b) Sheldrick, G. M. *SADABS*; University of Göttingen: Göttingen, Germany, 1998. (c) Beurskens, P. T.; Admiraal, G.; Beursken, G.; Bosman, W. P.; de Gelder, R.; Israel, R.; Smits, J. M. M. *DIRDIF94*; University of Nijmegen: Nijmegen, The Netherlands, 1994. (d) *teXsan*, version 1.11; Molecular Structure Corporation: The Woodlands, TX, 2000. (e) Palmer, D. *CrystalMaker*, version 7.0.4; CrystalMaker Ltd.: Yarnton, U.K., 2005.

Table 2. Selected Bond Distances (Å) and Coordination Volumes (Å^3)[a]

Pb1	S6	2.751(2)	In2	S5	2.517(2)
Pb1	S6	2.751(2)	In2	S5	2.517(2)
Pb1	S4	2.911(3)	In2	S7	2.576(3)
Pb1	S1	3.200(2)	In2	S9	2.604(3)
Pb1	S1	3.200(2)	In2	S8	2.7532(5)
Pb1	S7	3.255(2)	In2	S8	2.7532(5)
Pb1	S5	3.436(2)	average		2.620 (CN = 6)
Pb1	S5	3.436(2)	volume		23.83
average		3.118 (CN = 8)			
volume		52.38			
Pb2	S11	2.881(2)	In3	S11	2.503(3)
Pb2	S11	2.881(2)	In3	S7	2.584(2)
Pb2	S3	3.065(2)	In3	S7	2.584(2)
Pb2	S3	3.065(2)	In3	S8	2.7271(7)
Pb2	S10	3.107(2)	In3	S9	2.770(2)
Pb2	S10	3.107(2)	In3	S9	2.770(2)
Pb2	S9	3.310(3)	average		2.656 (CN = 6)
Pb2	S4	3.365(3)	volume		24.86
average		3.098 (CN = 8)			
volume		51.66			
Pb3	S11	2.887(2)	In4	S1	2.585(2)
Pb3	S11	2.887(2)	In4	S1	2.585(2)
Pb3	S4	3.038(2)	In4	S12	2.593(3)
Pb3	S6	3.121(2)	In4	S3	2.648(2)
Pb3	S6	3.121(2)	In4	S3	2.648(2)
Pb3	S7	3.194(3)	In4	S2	2.7302(7)
Pb3	S6	3.262(2)	average		2.632 (CN = 6)
Pb3	S6	3.262(2)	volume		24.01
average		3.097 (CN = 8)			
volume		52.19			
In1	S1	2.530(3)	In5	S5	2.479(3)
In1	S3	2.543(2)	In5	S10	2.517(3)
In1	S4	2.552(2)	In5	S12	2.572(2)
In1	S4	2.552(2)	In5	S12	2.572(2)
In1	S2	2.8105(5)	In5	S9	2.952(2)
In1	S2	2.8105(5)	In5	S9	2.952(2)
average		2.633 (CN = 6)	average		2.674 (CN = 6)
volume		24.08	volume		24.98
			In6	S10	2.625(2)
			In6	S10	2.625(2)
			In6	S10	2.625(2)
			In6	S10	2.625(2)
			In6	S12	2.636(2)
			In6	S12	2.636(2)
			average		2.629 (CN = 6)
			volume		24.00

[a] Under 3.5 Å with estimated standard deviations in parentheses for $Fe_{1.50}Pb_{5.50}In_{10}S_{22}$.

Results and Discussion

Synthesis and Characterization. The composition of this new compound was confirmed from SEM-WDS analyses to be $Fe_{1.47(5)}Pb_{5.48(3)}In_{10.10(7)}S_{22}$. TG-DTA measurements show that this compound, $Fe_{1.5}Pb_{5.5}In_{10}S_{22}$, melts congruently at 1098 K and recrystallizes at 1090 K, indicating a single-phase compound (Figure S1). Since there had been no report of Fe−Pb−In−S quaternary compounds, we had no information about the structure of the obtained compound. From the results of the XRD measurements, this new compound was deduced to be an isostructure of or a structure related to that of $Sn_{5.5}In_{11}S_{22}$.[12] Therefore, first of all, we assumed a compound, $Pb_{5.5}In_{11}S_{22}$, which would be a $Sn^{2+} \leftrightarrow Pb^{2+}$-exchanged compound of $Sn_{5.5}In_{11}S_{22}$, although $Pb_{5.5}In_{11}S_{22}$ has never been found even in the most recent peudobinary phase diagram, PbS−In_2S_3.[13] Next, we assumed that Fe atoms would be distributed at In sites in $Pb_{5.5}In_{11}S_{22}$. Our attempt to synthesis pure $Pb_{5.5}In_{11}S_{22}$ has been unsuccessful, which suggests that FeS would act as a mineralizer for the crystallization of a Pb-based compound with an $Sn_{5.5}In_{11}S_{22}$-type structure.

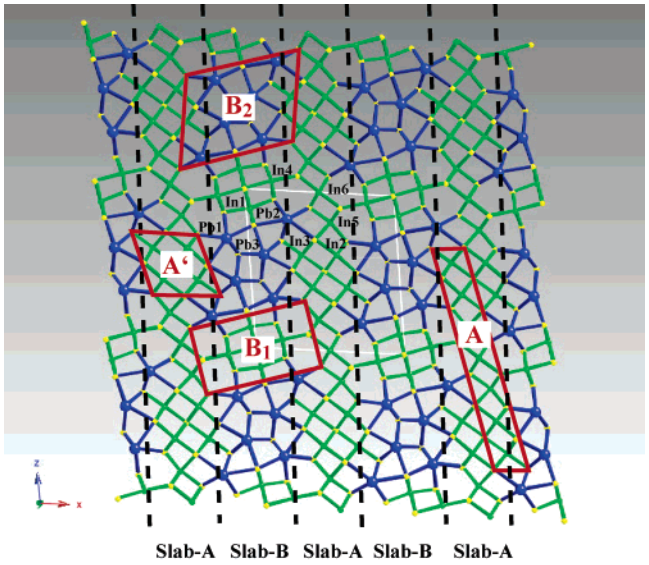

Figure 1. Crystal structure of $Fe_{1.5}Pb_{5.5}In_{10}S_{22}$, viewed parallel to [010] (blue circles, Pb; green circles, In; yellow circles, S). The structure is formed by two slabs (A and B). The ribbonlike substructure (A) is connected in a zigzag manner to form the A slab. The connected part (A′) has a SnS-type substructure. The B slab consists of two different substructures (B_1 and B_2) which are alternately connected along the *c* axis. There are 6 sites (In1−In6) for In. Fe atoms are mainly located at the In2 and In6 sites in the A slabs and at the In4 site in the B_1 substructures.

Details of Crystal Structure. The results of the single-crystal structure determination (Figure 1) reveal that the title compound is an isostructure of $Sn_{5.5}In_{11}S_{22}$ ($P2/m$)[12] and furthermore that the structure is closely related to the Pb_6-$In_{10}S_{21}$ structure ($C2/m$, Figure S2).[13] The structure of the title compound contains three lead sites with significantly distorted coordination spheres, which are trigonal prism-type structures with extra two ligands; each coordination number (CN) is eight. This specific feature of the coordination of lead ions is commonly observed in other multinary lead chalcogenides.[7,9,14] A quarter of an indium atom occupies the Pb1 site in an ordered manner. On the other hand, there is no crystallographically-independent site for the Fe atoms in the structure. At six indium sites, all of the Fe atoms are substituted randomly with various Fe/In ratios: 95.8:4.2 at In1, 71.0:29.0 at In2, 93.6:6.4 at In3, 85.8:14.2 at In4, 91.0:9.0 at In5, and 78.0:22.0 at In6. This manner of substitution

(12) Likforman, A.; Jaulmes, S.; Guittard, M. *Acta Crystallogr.* **1988**, *C44*, 1339.

(13) Krämer, V.; Berroth, K. *Mater. Res. Bull.* **1980**, *15*, 299.

(14) For example, see: (a) Skowron, A.; Brown, I. D. *Acta Crystallogr.* **1990**, *C46*, 527. (b) Skowron, A.; Brown, I. D. *Acta Crystallogr.* **1990**, *C46*, 531. (c) Skowron, A.; Brown, I. D. *Acta Crystallogr.* **1990**, *C46*, 534. (d) Skowron, A.; Brown, I. D. *Acta Crystallogr.* **1990**, *C46*, 2287. (e) Skowron, A.; Brown, I. D.; Tilley, R. J. D. *J. Solid State Chem.* **1992**, *97*, 199. (f) Matsushita, Y.; Takéuchi, Y. *Z. Kristallogr.* **1994**, *209*, 475. (g) Skowron, A.; Boswell, F. W.; Corbett, J. M.; Taylor, N. J. *J. Solid State Chem.* **1994**, *112*, 251. (h) Skowron, A.; Boswell, F. W.; Corbett, J. M.; Taylor, N. J. *J. Solid State Chem.* **1994**, *112*, 307. (i) Matsushita, Y.; Nishi, F.; Takéuchi, Y. In *Tropochemical Cell-Twinning*; Takéuchi, Y., Ed.; Terra Publishing: Tokyo, Japan, 1997.

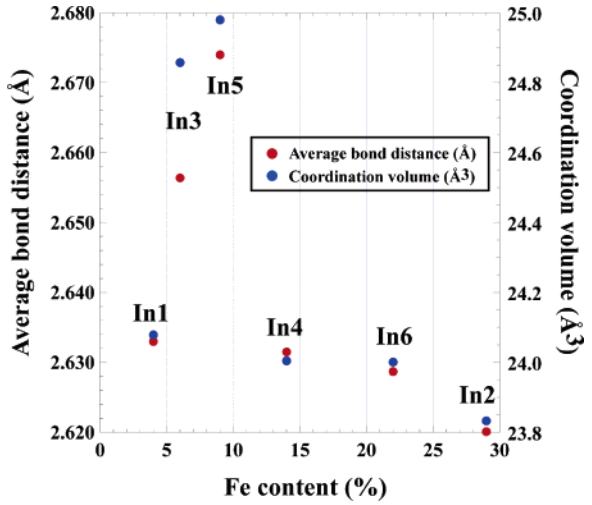

Figure 2. Fe-content dependence of average bond distance and coordination volume at each indium site in the $Fe_{1.5}Pb_{5.5}In_{10}S_{22}$ structure.

is understandable from a crystallochemical point of view that the ionic radii of In^{3+} and Fe^{2+} are very close: $r_{In^{3+}}^{CN=6} = 0.80$ Å and $r_{Fe^{2+}}^{CN=6,HS} = 0.780$ Å.[10] The coordination type of each indium site is a distorted octahedron, and the substitution of Fe little affects the coordination manner of the indium sites (Figure 2 and Table 2). Recently, Wang and Lee reported new $MPb_8In_{17}S_{34}$ (M = Cu, Ag, Au) compounds. In these crystal structures, M atoms are also substituted at the In sites.[15] On the other hand, the strong stereoactive lone-pair electrons of Pb^{2+} cause distortion modes at all of the cation sites (Table 2). The final refined composition is $Fe^{2+}_{1.48(2)}Pb^{2+}_{5.50}In^{3+}_{10.02(2)}S^{2-}_{22}$. This composition exactly keeps charge neutrality (charge variance = −0.02).

The structure has two kinds of slabs, A and B, running parallel to the *c* axis (Figure 1). The A slab contains a ribbon-shaped In−S substructure (A substructure, (InS) chain formed by 7 InS_6 octahedrons) similar to the Bi_2Te_3-like structure.[16] The (InS) chain (A substructure) is connected by two of the seven (InS) units at both ends to form the A slab. The connected part has a square-type substructure (A′) related to the SnS structure.[17] The B slab is formed from an alternating stack of two substructures (B_1 and B_2) along the *c* axis. The B_1 substructure, formed by In−S, is similar to the A′ substructure in the network, but it is a different shape. The B_2 substructure, formed by Pb−S, is more complex because of the active lone-pair electrons of Pb^{2+} (Figure 1). Similar networks can be seen in the $Pb_6In_{10}S_{21}$ structure[13] (Figure S2). Both compounds ($Fe_{1.5}Pb_{5.5}In_{10}S_{22}$ and $Pb_6In_{10}S_{21}$) have similar slab B substructures but differ in the network corresponding to slab A: a ribbon-shaped In−S substructure in $Pb_6In_{10}S_{21}$ is a (InS)-chain formed by six InS_6 octahedrons, and each (InS)-chain is connected with one of six (InS) units at both ends to form slab A. The connection

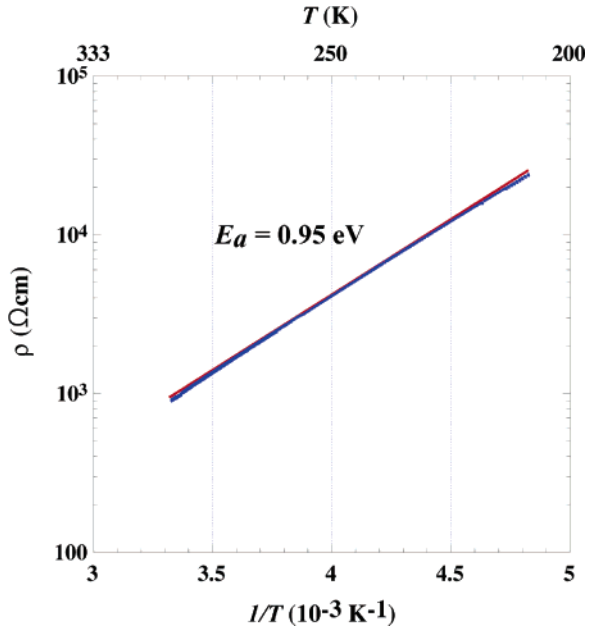

Figure 3. Arrhenius plot of electrical conductivity for a single crystal of $Fe_{1.5}Pb_{5.5}In_{10}S_{22}$. The blue line shows the observed data, and the red line represents the least-squares linear fit. The activation energy (E_a) is estimated to be 0.95 eV.

has a Sb_2S_3-like substructure[18] in $Pb_6In_{10}S_{21}$ instead of the SnS-type substructure in $Fe_{1.5}Pb_{5.5}In_{10}S_{22}$.

There are four crystallographically independent indium sites in $Fe_{1.5}Pb_{5.5}In_{10}S_{22}$ (In2, In3, In5 and In6) in the A slab and two sites (In1 and In4) in the B-slab, as shown in Figure 1. The Fe atoms are mainly located at the In2 and the In6 sites in the A slabs and at the In4 site in the B_1 substructures. All of these sites are strongly influenced by stereochemically active Pb^{2+}. On trial, we calculated the bond-valence sum for each site.[19] For the Pb1 site, the calculated valence, 2.161 is slightly larger than 2. This may be the result of partly substituted In^{3+} for Pb. However, we could not recognize any systematic influence of Fe substitution for the indium sites, which could be caused by the relatively low ratio of the substitution and the subtle ion-radius difference between In^{3+} and Fe^{2+}. The strong stereoactive lone-pair electrons of Pb^{2+} could give some over- or underestimated results in the bond-valence sum calculation.[20]

Physical Properties. $Fe_{1.5}Pb_{5.5}In_{10}S_{22}$ has metallic gray luster. From the electrical resistivity measurements, this compound is identified as a semiconductor. The band gap, E_a, estimated from the Arrhenius plot of the data is 0.95 eV (Figure 3). The temperature (*T*) dependence of the molar magnetic susceptibility (χ_M) is shown in Figure 4. No anomaly is observed down to 2 K in $\chi-T$ curve. There is no difference of magnetic susceptibility between the ZFC and FC measurements at 0.5 T. In the temperature range above 100 K, the paramagnetic susceptibility obeys a Curie−Weiss (CW) law with a constant term, χ_0. The parameters obtained from the fitting are Curie constant: C_{Curie} =

(15) Wang, K.-C.; Lee, C.-S. *Inorg. Chem.* **2006**, *45*, in press.
(16) Feutelais, Y.; Legendre, B.; Rodier. N.; Agafonov, V. *Mater. Res. Bull.* **1993**, *28*, 591.
(17) (a) For a low-temperature form SnS, see: del Bucchia, S.; Jumas, J. C.; Maurin, M. *Acta Crystallogr.* **1981**, *B37*, 1903. (b) For a high-temperature form SnS, see: von Schnering, H. G.; Wiedemeier, H. *Z. Kristallogr.* **1981**, *156*, 143.
(18) Kyono, A.; Kimata, M.; Matsuhisa, M.; Miyashita Y.; Okamoto, K. *Phys. Chem. Mineral.* **2002**, *29*, 254.
(19) Brown, I. D.; Altermatt, D. *Acta Crystallogr.* **1985**, *B41*, 244.
(20) Wang, X.; Liebau, F. *Z. Kristallogr.* **1996**, *211*, 437.

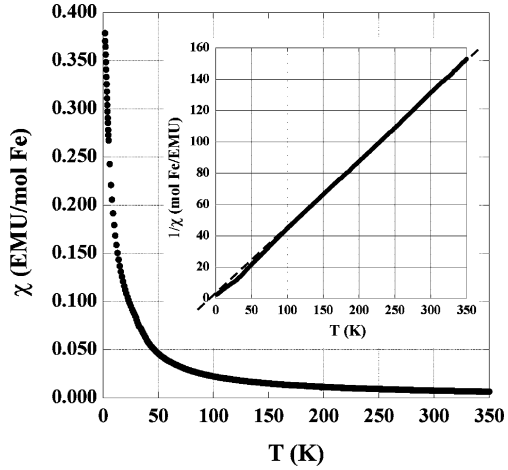

Figure 4. Temperature (T) dependence of magnetic susceptibility (χ) measured in ZFC using polycrystalline $Fe_{1.5}Pb_{5.5}In_{10}S_{22}$. The inset shows a χ^{-1} vs T plot. The dotted line represents a Curie−Weiss fit.

2.422(7) emu K/mol Fe, Weiss temperature (Θ_{CW}) = −21.0(3) K, and χ_0 = 0.00008(2) emu/mol. The negative Θ_{CW} value suggests that some antiferromagnetic interactions exist between the magnetic Fe ions. The effective magnetic moment, p_{eff}, estimated from the C_{Curie}, is 4.40 μ_B, which suggests that Fe^{2+} takes a high-spin state ($t_{2g}^4e_g^2$, $S = 2$) in this compound, although it is slightly lower than the calculated p_{eff} (4.90 μ_B) for a high-spin Fe^{2+}.[21] This is consistent with the results from the crystallographic analyses mentioned above. These results indicate that $Fe_{1.5}Pb_{5.5}In_{10}S_{22}$ has an antiferromagnetic interaction among the Fe^{2+} ions but is paramagnetic at least down to 2 K without any magnetic orderings.

Summary

We obtained a new compound, $Fe_{1.5}Pb_{5.5}In_{10}S_{22}$, in the Fe−Pb−In−S system. This compound melts at 1098 K congruently and recrystallizes at 1090 K. The crystal structure is an isostructure with $Sn_{5.5}In_{11}S_{22}$, and is related to the $Pb_6In_{10}S_{21}$ structure. The structure is formed by two different types of slabs (A and B) similar to those in $Pb_6In_{10}S_{21}$. The A slab contains a ribbonlike Bi_2Te_3-type substructure (A), and each A substructure is connected in a zigzag manner, forming a substructure (A′) at the connected part. The B slab is formed by alternating substructures (B_1 and B_2). The B_1 substructure, formed by In and S, has a structure similar to that of A′. The B_2 substructure is formed by Pb and S. In the structure, Fe atoms are substituted for the six indium sites with various Fe/In ratios. The substitution of Fe for In seems to not the coordination type. Both the lead and indium sites have distorted coordinations. The strong stereoactive lone-pair electrons of Pb^{2+} mainly cause the significant distortion of the coordination sphere. In the electrical resistivity measurements, $Fe_{1.5}Pb_{5.5}In_{10}S_{22}$ shows a semiconducting behavior with a band gap of 0.95 eV. This compound shows a CW-type paramagnetism. The magnetic ions, Fe ions in this compound, are Fe^{2+} with a high spin state ($t_{2g}^4e_g^2$, $S = 2$); the dominant magnetic interaction between the Fe^{2+} ions is antiferromagnetic, but magnetic ordering is not observed at least down to 2 K.

Acknowledgment. The authors thank to Dr. J. Yamaura for support in the single-crystal X-ray diffraction measurements using a CCD diffractometer. This work is partly supported by Grants-in-Aid for Scientific Research (No. 407 and No. 758) and for Creative Scientific Research (No. 13NP0201) from the Ministry of Education, Culture, Sports, Science, and Technology. We also gratefully acknowledge Komatsu Ltd. Co. for financial support.

Supporting Information Available: Crystallographic files in CIF format for $Fe_{1.5}Pb_{5.5}In_{10}S_{22}$ and two figures (Figure S1 and S2). This material is available free of charge via the Internet at http://pubs.acs.org.

IC0515296

(21) West, A. R. *Solid State Chemistry and Its Applications*; John Wiley & Sons: Chichester, U.K., 1984.